Remote Sensing of Environment 286 (2023) 113420

Contents lists available at ScienceDirect

Remote Sensing of Environment

journal homepage: www.elsevier.com/locate/rse

A spatially varying model for small area estimates of biomass density across the contiguous United States

Paul May [a,*], Kelly S. McConville [b], Gretchen G. Moisen [c], Jamis Bruening [a], Ralph Dubayah [a]

[a] University of Maryland - College Park, College Park, MD, United States
[b] Harvard University, Cambridge, MA, United States
[c] Rocky Mountain Research Station, U.S. Department of Agriculture (USDA) Forest Service, Ogden, UT, United States

ARTICLE INFO

Keywords:
Small area estimation
Forest biomass
Spatial modeling
Bayesian
Area-level

ABSTRACT

The USDA Forest Service, Forest Inventory and Analysis (FIA) program constructs area estimates of forest attributes through a quasi-systematic sample of field plots distributed across the contiguous US. The program is under increasing pressure to provide estimates over small areas, for which the precision of FIA estimates is limited by small sample sizes. Small area estimation (SAE) models can improve the precision of estimates by leveraging relationships between forest attributes and auxiliary data across multiple small areas of interest. SAE models with large model domains are challenged by requiring auxiliary data encompassing the large domain and by spatially varying relationships between the auxiliary data and forest attributes. We implement a Fay–Herriot SAE model that accounts for spatial variation to make estimates of forest above-ground biomass density (AGBD) within 64,000 hectare hexagons across the contiguous US. Model inference is conducted through a Bayesian paradigm, providing AGBD estimates and quantification of uncertainty through posterior standard deviations and credible intervals. We compare the utility of data from the Global Ecosystem Dynamics Investigation (GEDI) and the National Land Cover Database 2016 Tree Canopy Cover (TCC) product as auxiliary data within the model. Results show that models using GEDI data provide more precise estimates of AGBD than direct estimates using FIA plot data alone while giving accurate quantification of uncertainty. The model using only the TCC product as auxiliary data also reported more precise estimates, but a cross-validation study revealed the reported uncertainty to be overly optimistic for high-biomass areas. We demonstrate that accounting for spatial variation in the model is crucial, and that doing otherwise leads to poor quantification of uncertainty and locally biased estimates. This study not only provides an effective model for small area estimates of AGBD with a large model domain, but also emphasizes the importance of validating models and their reported errors.

1. Introduction

The USDA Forest Service, Forest Inventory and Analysis (FIA) program monitors the status of forests across the US through a quasi-systematic sample of field plots (Bechtold and Patterson, 2005). For each field plot, important forest attributes such as average biomass, tree density, and diameter at breast height are directly measured or estimated through a combination of measurements and allometric equations. FIA maintains over 300,000 field plots across the contiguous United States (CONUS), approximately one plot per 6000 acres, allowing precise estimates of forest attribute population averages over large areas through direct, design-based statistical estimates. The estimates are direct in the sense that within a given area, only the plot-sampled forest attributes within the area are used as statistical variables to make an estimate, though auxiliary information such as aerial imagery may be used to post-stratify the samples. The estimates are design-based in the sense that the assumed-random selection of the plot locations, i.e., the sampling design, is used to drive statistical inference. Direct, design-based methods have the virtue of only making assumptions about the sampling design, which is known *a priori*, and not about the distribution of the forest attributes, which may be complex and difficult to model. Direct, design-based methods suffer the drawback of their precision being dependent on the sample size within a given area.

There are increasing needs for FIA to provide estimates of forest attributes over smaller areas (Prisley et al., 2021; Wiener et al., 2021). Small areas with few sampled plots will yield direct estimates with unacceptably high variance, providing little information on the average

* Corresponding author.
E-mail addresses: pbmay@umd.edu (P. May), kmcconville@fas.harvard.edu (K.S. McConville), gretchen.g.moisen@usda.gov (G.G. Moisen), jamis@terpmail.umd.edu (J. Bruening), dubayah@umd.edu (R. Dubayah).

https://doi.org/10.1016/j.rse.2022.113420
Received 2 August 2022; Received in revised form 18 November 2022; Accepted 16 December 2022
Available online 22 December 2022
0034-4257/

forest attribute within the area. Note our use of 'small' or 'large' to describe an area has no fixed geographic meaning, but rather implies whether the sample size within an area is large enough to produce precise direct estimates. Because field samples are expensive and laborious to collect, simply intensifying the sampling density until the desired precision is achieved is rarely practical.

Small area estimation (SAE) models assume a linking regression model relating the target variable to auxiliary data that is, ideally, strongly correlated with and more densely sampled than the target variable (Rao and Molina, 2015). The linking model assumes a relationship that is stable across a greater domain, borrowing strength in order to increase the effective sample size for the small areas. SAE models can greatly improve precision over the direct estimates. The cost is the introduction of model assumptions, including the assumed functional relationship between the target and auxiliary variables and the assumed distribution of the model errors. This necessitates careful model criticism and validation. It also fundamentally changes the statistical paradigm through which estimates are made, considering the sampled units to be stochastic, instead of the sampled locations (Särndal et al., 1978; Gregoire, 1998).

SAE models can be partitioned into area-level and unit-level models. Area-level models assume a linking equation at the level of the small areas, where area aggregates of the target variable are regressed against area-level auxiliary data. Unit-level models assume a linking equation at the level of the individual sampled units, in our case, the field plots. While unit-level models potentially leverage a richer source of information, in practice they are more challenging to implement, due to the more complex distributions and relationships at the unit level, the difficulty of obtaining unit-level auxiliary data, and sometimes computational issues.

The use of SAE models in forestry has rapidly increased in the past two decades due to the wide availability of remote sensing data to serve as auxiliary data. Ver Planck et al. (2018), White et al. (2021), Temesgen et al. (2021), Cao et al. (2022) implemented area-level models to estimate forest attributes. Breidenbach et al. (2018), Green et al. (2020) implemented both area-level and unit-level models, comparing the performance of the models. Geostatistical models have also been used (Babcock et al., 2018), where spatial misalignment of the field plot and auxiliary data is reconciled by simultaneously interpolating both in a linear coregionalization model. Geostatistical methods are computationally intensive and typically assume accurate geolocation of both data sources.

Many implementations of forestry SAE models in the literature are limited in spatial scope, making estimates for a handful of small areas within the greater area of a state, ecoregion or national forest. While this may sometimes be due to interest being limited to the particular study area, there are certainly challenges in expanding SAE models to large encompassing domains. One challenge is availability of auxiliary data across large areas. For instance, a popular auxiliary data source is airborne lidar data (Ver Planck et al., 2018; Babcock et al., 2018; Green et al., 2020; Temesgen et al., 2021), where individual airborne lidar collections are often limited in scope. A second challenge is that borrowing strength, i.e., assuming a constant regression model, across too large of an area will introduce local bias and unmodeled uncertainty, as functional relationships between auxiliary and target variables often vary over space. White et al. (2021) made small area estimates of forest attributes across the Interior West of the United States by segmenting the region into ecosections believed to be homogeneous, fitting a unique model to each, using the National Land Cover Database (NLCD) 2016 Tree Canopy Cover (TCC) map (Coulston et al., 2012; Yang et al., 2018) as auxiliary data. If the aforementioned challenges can be surmounted, fitting a single model that accounts for spatial variation across a large encompassing domain containing many small areas is attractive, as it enables national forest inventories to produce small area estimates across a country with a single consistent model, avoiding the need to partition the country into separate model domains. Such partitioning is rarely data-driven, but instead uses pre-drawn political or ecosystem boundaries out of necessity. Spatially varying models have been demonstrated to be effective when linking forestry and remote sensing data over large domains (Finley et al., 2011; Datta et al., 2016). In particular, Datta et al. (2016) used a spatially varying model relating FIA plot observations of forest biomass to satellite-derived Normalized Difference Vegetation Index across CONUS, showing the relationship between the variables to change substantially over space.

Here we implement an area-level SAE model that includes a spatial random error and spatially varying regression coefficients to estimate above ground biomass density (AGBD) within 64,000 ha hexagons across CONUS. For auxiliary data, we compare predictors derived from the Global Ecosystems Dynamics Investigation (GEDI; Dubayah et al., 2020a) and the NLCD 2016 TCC product. We conduct inference through a Bayesian paradigm that accounts for uncertainty in all model parameters and effects in the downstream estimates of AGBD. We show through a cross-validation study that the models using GEDI data produce reliable credible intervals for AGBD while yielding lower uncertainty than the direct estimates. The model that used the TCC product alone reported the lowest standard deviations, but yielded unreliable credible intervals in high-biomass areas. Accounting for spatial variation in the model was found to be crucial, and neglecting it resulted in local biases and unreliable credible intervals. This study is meant not only to illustrate an effective SAE model for AGBD, but also to provide a cautionary example about the importance of validating SAE models and their reported errors.

2. Data and methods

2.1. FIA data and hexagon map

FIA maintains a quasi-systematic sample, which the program assumes to be approximately random, of over 300,000 field plots throughout CONUS. Through the field plots and design-based statistical methods, FIA produces estimates of area population averages/totals of the forest attributes. Field plots are visited on a five-year cycle for the eastern US and a ten-year cycle for the western US. The most recent ten-year cycle, providing a potential sample at every field plot within CONUS (some plots are not visited due to access issues), occurred over the years 2009–2019. The sampling design and estimation methods are described extensively in Bechtold and Patterson (2005). FIA uses post-stratification as an estimation method, where aerial or satellite imagery is used as a stratification layer to partition the area of interest into more homogeneous classes. The motivation for the stratification is to separate the field samples into less internally variable classes, hopefully reducing the variance of the direct estimates.

Menlove and Healey (2021) produced an AGBD map for CONUS using FIA data from 2009–2019 and post-stratification estimates. The areas of estimation are 64,000 ha hexagons, with 12,591 hexagons total, containing on average 26 field plots per hexagon. The standard errors of the hexagon direct estimates can be substantial, especially for high-biomass areas. We use these hexagons as the small areas and CONUS as the greater domain. For direct estimates, we use the Horvitz–Thompson estimators (Horvitz and Thompson, 1952). Let μ_j be the true, unknown AGBD for hexagon j. The Horvitz–Thompson estimate $\hat{\mu}_j$ and associated estimate variance are:

$$\hat{\mu}_j = \frac{1}{n_j}\sum_{i=1}^{n_j} y_{ij} \tag{1}$$

$$\hat{\sigma}_j^2 = \widehat{\mathrm{Var}}[\hat{\mu}_j] = \frac{1}{n_j(n_j-1)}\sum_{i=1}^{n_j}(y_{ij}-\hat{\mu}_j)^2 \tag{2}$$

for hexagons $j = 1, \dots, N$, where y_{ij} is a field plot AGBD measurement and n_j is the number of field plots in hexagon j. The direct estimates are generated using FIA plots from 2009–2021, as this timespan contains the most recent complete FIA sampling cycle for CONUS,

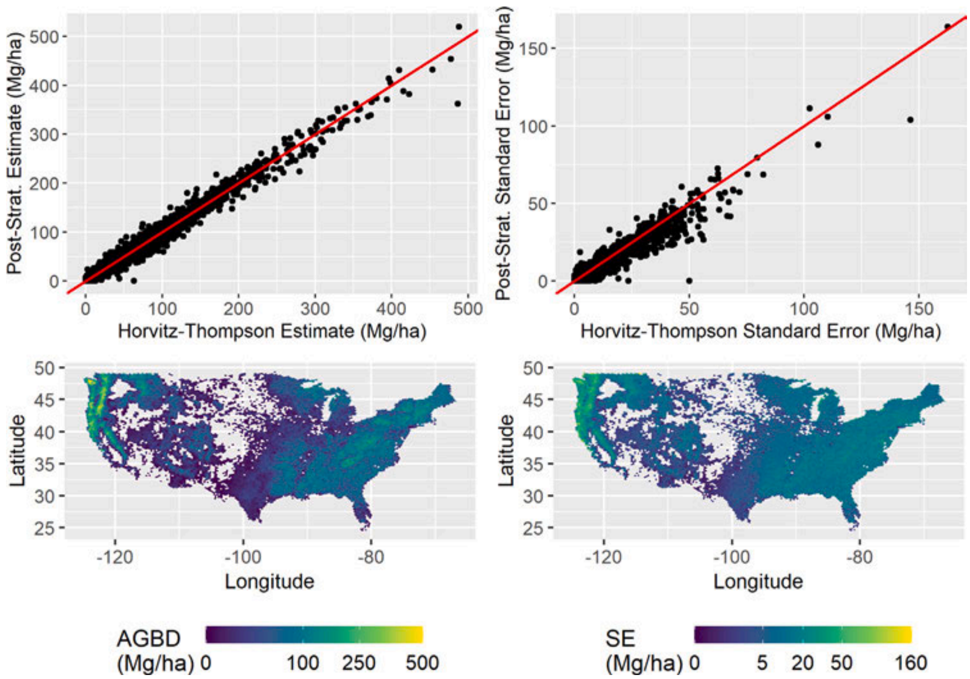

Fig. 1. The top row gives the Horvitz–Thompson estimates and standard errors versus the post-stratification estimates and standard errors in Menlove and Healey (2021) with one-to-one lines in red. The two sets of estimates are comparable, but the Horvitz–Thompson estimates are easier to reproduce. The bottom row gives spatial maps of the Horvitz–Thompson direct estimates and standard errors across the 9793 hexagons of area 64,000 ha used in this study.

using the most recent sample for each individual plot. We use the Horvitz–Thompson estimator because the estimates are comparable to the post-stratification estimates in Menlove and Healey (2021) and it makes reproducing results easier (Fig. 1, top row). Because the quasi-systematic sampling design of FIA can be approximated by a simple random sampling design (Bechtold and Patterson, 2005, p. 25), the above Horvitz–Thompson estimator provides appropriate design-based estimates. Hereafter, we will refer to the Horvitz–Thompson estimates as the direct estimates. We omit hexagons with a AGBD direct estimate of 0 Mg/ha, as these necessarily have a standard error of zero, making the model presented in Section 2.4 ill-defined. This leaves $N = 9783$ positive-biomass hexagons to be used in this study. The bottom row of Fig. 1 gives a spatial map of these hexagons, their direct estimates and their standard errors.

2.2. GEDI area predictor

We use spaceborne lidar data from GEDI to produce an area predictor of AGBD. GEDI is a lidar instrument onboard the International Space Station that has been collecting observations of vertical vegetation structure since 2019 (Dubayah et al., 2020a). Laser pulses illuminate 25 m diameter circular footprints on the ground, returning the reflected waveform to the instrument. Above ground vegetation reflects the emitted pulse, encoding the returned waveform with information on the vertical distribution of vegetation. From the waveform, important vegetation metrics can be derived, such as canopy height, canopy cover and the relative height (RH) metrics. The RH metrics are quantile statistics, giving the height above ground below which a given percentage of the waveform energy was reflected. GEDI collects footprint waveforms along 8 parallel ground transects, with a 60 m footprint spacing center-to-center along transect, and 600 m between transects. While GEDI does not provide wall-to-wall, or spatially complete, observations, the sampled footprints are dense, with on average approximately 100,000 quality footprints per 64,000 ha hexagon.

The GEDI L2A data product provides footprint observations of ground elevation and RH metrics (Dubayah et al., 2020b). The L2A product has a quality flag to identify potentially poor footprint returns. We use this quality flag as an initial filter. We use RH95 as our footprint metric, as it gives a measure of the canopy height without being overly sensitive to noise. To produce a hexagon-level predictor of AGBD, within each hexagon we take the average squared RH95 value for every footprint at least partially overlapping a 30 m pixel classified as forest by the NLCD 2019 Land Cover Map (Dewitz, 2021). This quantity is multiplied by the proportion of forest classified pixels. To be precise, let g_{ij} be the ith observation of RH95 within hexagon j overlapping a forest pixel, and let $P_j \in [0,1]$ be the proportion of forest pixels within the hexagon. Then the GEDI predictor for hexagon j is

$$X_{G,j} = \frac{P_j}{n_{G,j}} \sum_{i=1}^{n_{G,j}} g_{ij}^2 \tag{3}$$

where $n_{G,j}$ is the number of forest-overlapping GEDI footprints in hexagon j. The rationale is that squaring RH95 values g_{ij} accounts for the non-linear relationship between canopy height and biomass, while filtering by forest class omits GEDI height measurements that are not representative of trees. Fig. 2 plots the relationship between the GEDI predictors of Eq. (3) and the direct estimates of AGBD. The plot suggests a strong linear relationship between the GEDI predictor and AGBD.

2.3. NLCD tree canopy cover predictor

The second area predictor used in this study is data from the NLCD 2016 TCC product (Coulston et al., 2012; Yang et al., 2018). The TCC product was derived from Landsat 8 data, using a random forest model to make 30 m pixel resolution predictions of tree canopy cover, ranging from 0%–100%, across CONUS. White et al. (2021) used the average canopy cover pixel-value within each small area as a predictor for forest attributes across the Interior West of the US. We use this same predictor for the hexagons across CONUS, rescaling the percentage to a proportion, from 0–1. Fig. 2 plots the relationship between the TCC predictor and the direct estimates of AGBD. While the majority of the point-pairs fall into a linear relationship, there is substantial upward leakage, especially at high biomass hexagons. A similar relationship is seen in White et al. (2021, Figure 5). Indeed, the linear portion of the relationship reaches a maximum at around 100 Mg/ha, while the

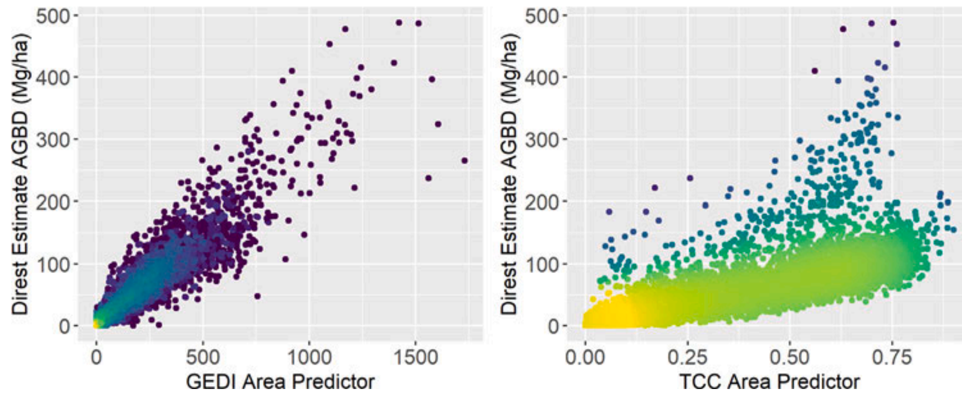

Fig. 2. GEDI predictor (left) and TCC predictor (right) versus direct estimates of AGBD for all hexagons. Brighter colors indicate a higher density of points. (For interpretation of the references to color in this figure legend, the reader is referred to the web version of this article.)

remaining variation in direct estimates, ranging to almost 500 Mg/ha, falls completely outside this line. This contrasts sharply with the GEDI predictor, where the linear relationship seems to span the entire range of AGBD direct estimates. We could not find any transformation that improved the relationship between the TCC predictor and the AGBD direct estimates.

2.4. Spatial Fay–Herriot model

The precision of direct estimates is proportional to the sample size within the domain, which is problematic for small areas containing few FIA field plots. This motivates borrowing strength from auxiliary data by assuming some consistent relationship between predictors derived from auxiliary data and the population means. The Fay–Herriot model (Fay and Herriot, 1979) is an area-level SAE model that posits (1) an unbiased relationship between the direct estimates and the population mean, and (2) a linear relationship between the population mean and area-level auxiliary data. Recall that for hexagons $j = 1, \ldots, N$, we define μ_j as the unknown AGBD for hexagon j and $\hat{\mu}_j$ as the direct estimate with variance $\hat{\sigma}_j^2$. Further, let $X_{k,j}$; $k = 1, \ldots, p$ be the p different area-level predictors. For our study, we either use the GEDI or TCC predictor alone ($p = 1$) or both the GEDI and TCC predictors ($p = 2$). The traditional Fay–Herriot model can be written as

$$\hat{\mu}_j = \mu_j + \delta_j, \qquad \delta_j \sim N(0, \hat{\sigma}_j^2) \tag{4}$$

$$\mu_j = \mu_0 + \sum_{k=1}^{p} X_j \beta_k + \epsilon_j, \qquad \epsilon_j \sim N(0, \sigma_\epsilon^2) \tag{5}$$

for $j = 1, \ldots, N$, where δ_j is the sampling error between the direct estimate and true biomass density, μ_0 and $\beta_k;\ k = 1, \ldots, p$ are the regression intercept and coefficients respectively, and $\epsilon_j;\ j = 1, \ldots, N$ are independently distributed model errors, representing variation in AGBD not explained by the linear relationship with the predictor. Direct estimate variances $\hat{\sigma}_j^2$ are assumed known and fixed, but the remaining parameters are unknown and inferred from the data. While direct estimate $\hat{\mu}_j$ uses only plot data within small area j, regression parameters $\sigma_\epsilon^2,\ \mu_0,\ \beta_1, \ldots, \beta_p$ are global parameters, and are estimated using data throughout the greater domain. If uncertainty in the regression line is less than that of the direct estimates, the Fay–Herriot model can provide more precise estimates. However, if the model is misspecified, the model can produce biased estimates and erroneous inference. A possible cause of misspecification is spatial variation in the process not captured by the model. Unmodeled spatial variation in the process can cause poor quantification of uncertainty and local bias, where a 'globally' unbiased model will underestimate the target variable in some locales and overestimate in others. To model spatial variation, we use a spatial Fay–Herriot model (SFH), which is identical to Eqs. (4) and (5), except regression Eq. (5) is replaced with

$$\mu_j = \mu_0 + \sum_{k=1}^{p} X_{k,j}(\beta_k + \tilde{\beta}_{k,j}) + \eta_j + \epsilon_j, \tag{6}$$

which now includes mean-zero spatial random coefficients $\tilde{\beta}_{k,j}$ and mean-zero spatial random error η_j. These random effects provide a smooth spatial adjustment to the regression coefficients and the model intercept respectively. The spatial variation of these adjustments is inferred from the data. Most applications of a spatial Fay–Herriot model consider only the spatial error η_j (Pratesi and Salvati, 2008; Marhuenda et al., 2013; Ver Planck et al., 2018); far fewer use a spatially varying regression coefficient (Chandra et al., 2015). However, we found this to be crucial for our application. The spatially varying regression coefficient can also be interpreted as a heteroskedastic spatial error, as

$$\mathrm{Var}[X_{k,j}\tilde{\beta}_{k,j}] = X_{k,j}^2 \mathrm{Var}[\tilde{\beta}_{k,j}], \tag{7}$$

meaning the variance increases quadratically with increases in predictor $X_{k,j}$. Results in Section 3.2 show that removing the spatial regression coefficient resulted in overly optimistic standard deviations at high-biomass areas, which is sensible within this interpretation. Eq. (7) also illustrates a particular caution that must be taken with spatially varying coefficients, which is noted in the original developing paper (Gelfand et al., 2003): spatially varying coefficients are likely only appropriate if $X_{k,j} > 0$. Predictors that take on both negative and positive values will result in a U-shaped variance pattern centered around zero, which seems rarely justifiable. This means the common practice of centering predictors prior to model fitting is ill-advised here.

We model the spatial effects $\tilde{\beta}_{k,j},\ \eta_j$ as mean-zero Gaussian processes (Cressie, 2015, Chapter 2.3) with Matèrn covariance functions (Genton, 2001, Equation 12). Focusing on η_j for ease of exposition, this implies the joint distribution of $\eta_j;\ j = 1, \ldots, N$ across all hexagons is multivariate normal with zero mean and covariance matrix determined by the Matèrn covariance function. The Matérn covariance function assigns covariances between hexagons based on the distance between the hexagon centers, where covariance decreases as the distance increases. In particular, let s_j be the location for the center of hexagon j and $C_\eta(\cdot)$ be the Matérn covariance function for η_j. Then

$$\vec{\eta} = \begin{bmatrix} \eta_1 \\ \vdots \\ \eta_N \end{bmatrix} \sim \mathrm{MVN}\left(\vec{0}, \boldsymbol{\Sigma}_\eta\right); \quad \text{where} \quad [\boldsymbol{\Sigma}_\eta]_{ij} = C_\eta(\|s_i - s_j\|) \tag{8}$$

and where $\|s_i - s_j\|$ is the distance between the hexagon centers. The Matérn covariance function depends on a smoothness parameter, a variance parameter, and a range parameter. The smoothness parameter is typically fixed at the outset and not estimated from the data. The variance parameter σ_η^2 controls the constant variance of η_j, i.e. $\sigma_\eta^2 = \mathrm{Var}[\eta_j]$ for all $j = 1, \ldots, N$. The range parameter ϕ_η controls the rate at which covariance decays with distance. Larger range values imply slower covariance decay, resulting in a spatial effect that varies slowly over space. Fig. 3 gives two computer-simulated Gaussian processes over hexagons in the state of Oregon with different Matérn range

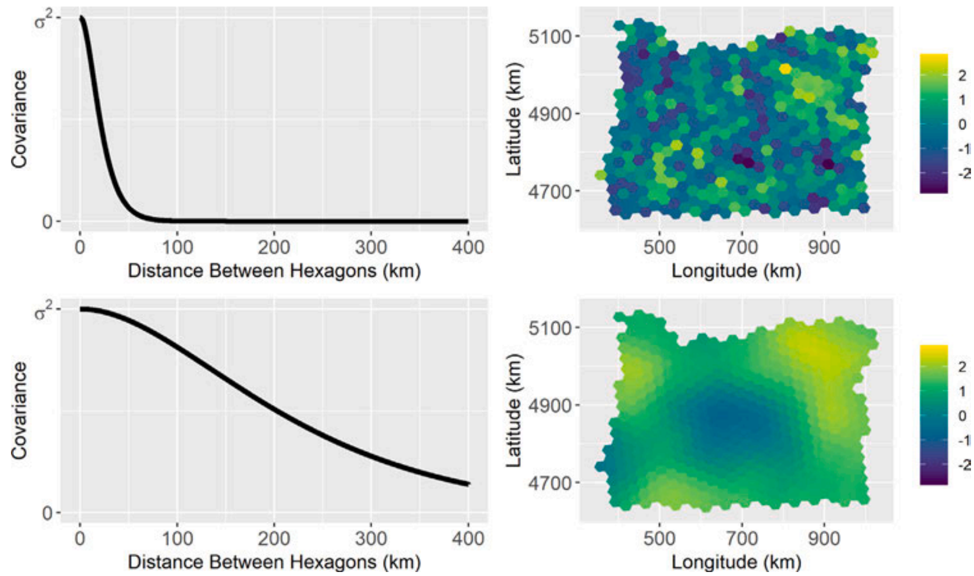

Fig. 3. Computer simulated Gaussian processes (right) with Matérn covariance functions (left) over hexagons within the state of Oregon. The top row has range $\phi = 10$ km and the bottom row has range $\phi = 100$ km. Larger range parameters produce slower decay of spatial covariance. Both processes have variance $\sigma^2 = 1$ and smoothness $\nu = 2$.

parameters to help visualize the parameters effect on the model. Each spatial effect $\eta_j,\ \tilde{\beta}_{1,j},\ldots,\tilde{\beta}_{p,j}$ is given a Matèrn covariance function with variance parameters $\sigma^2_\eta,\ \sigma^2_{\beta,1},\ldots,\sigma^2_{\beta,p}$ respectively and range parameters $\phi_\eta,\ \phi_{\beta,1},\ldots,\phi_{\beta,p}$ respectively, which are estimated from the data. All Matèrn covariance functions are assigned a fixed smoothness parameter $\nu = 2$.

2.5. Bayesian estimation with R-INLA

The SFH model (6) has unknown parameters $\theta = [\mu_0,\ \sigma^2_\epsilon,\ \sigma^2_\eta,\ \phi_\eta,\ \beta_1,\ \sigma^2_{\beta,1},\ \phi_{\beta,1},\ldots,\beta_p,\ \sigma^2_{\beta,p},\ \phi_{\beta,p}]^T$ and unknown hexagon AGBDs $\mu_j;\ j = 1,\ldots,N$. We employ a Bayesian method of estimation, deriving posterior distributions for all model parameters. In particular, we are interested in the marginal posterior distribution for hexagon AGBD values, μ_j:

$$p(\mu_j|\text{data}) = \int_\Theta p(\mu_j|\theta,\text{data})\cdot p(\theta|\text{data})\ d\theta \tag{9}$$

$$\propto \int_\Theta p(\mu_j|\theta,\text{data})\cdot f(\text{data}|\theta)\cdot \pi(\theta)\ d\theta, \tag{10}$$

where $f(\text{data}|\theta)$ is the data likelihood and $\pi(\theta)$ is the prior distribution on the model parameters, integrating across the entire parameter space $\theta \in \Theta$. The posterior distribution for μ_j summarizes the probability of AGBD values within hexagon j given the observed data. From the posterior AGBD, $p(\mu_j|\text{data})$, we compute point estimates as the posterior mean, $\text{E}[\mu_j|\text{data}]$, and error estimates as the posterior standard deviation, $\sqrt{\text{Var}[\mu_j|\text{data}]}$. Also useful are credible intervals, giving an interval that contains the unobserved hexagon AGBD with a given probability. For example, $[a_j,\ b_j]$ is a 95% credible interval for μ_j if

$$\text{Prob}[a_j < \mu_j < b_j] = 0.95. \tag{11}$$

Credible intervals are non-unique, as a_j, b_j could be set to the 2.5%, 97.5% quantiles of posterior $p(\mu_j|\text{data})$, or the 1%, 96% quantiles, both resulting in 95% credible intervals. We use the highest posterior density interval (HPDI), which is the credible interval with the shortest length. Because posteriors for μ_j are approximately normal and symmetric, this is effectively equivalent to choosing equal-tail intervals (2.5%, 97.5% posterior quantiles for a 95% credible interval).

Typically, the integrals involved in computing the marginal posteriors ((9),(10)), and summary statistics from these posteriors, are intractable. A common solution is to employ Markov Chain Monte Carlo (MCMC) methods to draw samples from the joint posterior. Desired quantities can be computed from these samples. We instead implement Integrated Nested Laplace Approximations (INLA) through the 'R' package 'R-INLA', allowing fast and accurate Bayesian inference without MCMC sampling (Rue et al., 2009; Lindgren and Rue, 2015; R. Core Team, 2021). INLA is a method for Bayesian inference designed for latent Gaussian models. The SFH model is a latent Gaussian model because all of the latent, or unobserved, effects are normally distributed. Fay–Herriot models, spatial or otherwise, are straight-forward to implement in R-INLA.

As alluded to, Bayesian inference requires specification of a prior distribution $\pi(\theta)$ on the model parameters, describing prior belief on reasonable parameter values. We assigned independent, uninformative priors to each individual parameter, though because the sample size is so large (9783 positive biomass hexagons) relative to the number of model parameters (at most 10, if both GEDI and TCC are used as predictors), the posterior distribution for μ_j is insensitive to any reasonable choice of priors.

2.6. Model assessment and validation

The objective of SAE models is to produce more precise estimates than the direct estimates over small areas. Therefore an intuitive assessment of the model is to compare model posterior standard deviations to the standard error of the direct estimates. Note that this comparison is made between the products of two different statistical paradigms: the posterior standard deviation is a Bayesian, model-based concept, describing the expected deviation of the unobserved, assumed-random population AGBD from the posterior mean, as given by the posterior distribution. The standard error of the direct estimate is a design-based concept, describing the expected deviation of the estimate upon resampling (random selection of new plot locations) from the assumed-fixed population AGBD. An adequate comparison of the two paradigms is outside the scope of this work and the abilities of the authors, but the interested reader is referred to Gregoire (1998). We only point out that the comparison of model-based and design-based uncertainties is ubiquitous in the SAE literature, and that in practice, the posterior standard deviations and direct-estimate standard errors will be interpreted similarly: as a scalar measure of uncertainty for the population estimate.

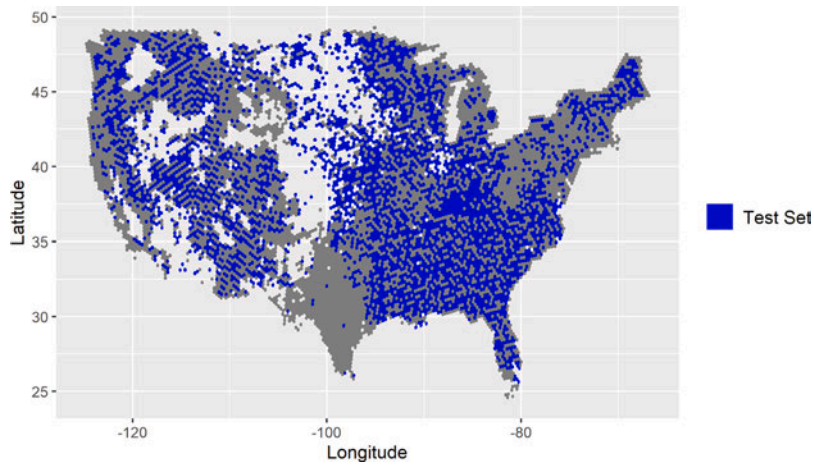

Fig. 4. Spatial distribution of the test hexagons (hexagons with a sample size greater than 26) used in the cross-validation study.

The comparison of standard deviations/errors can be done not only in terms of absolute magnitude, but also relative magnitude. The coefficient of variation (CV) of an estimate is the standard deviation/error of the estimate divided by the estimate itself, giving the proportional magnitude of the error relative to the estimate. The CV is unstable for estimate values close to zero, so we restrict our CV comparisons to hexagons with a direct estimate greater than 50 Mg/ha. We also examine the effective increase in sample size, i.e. the number of additional field samples per hexagon that would need to be collected to achieve the same precision via the direct estimate,

$$\mathrm{ESI}_j = \frac{\hat{\sigma}_j^2}{\mathrm{Var}[\mu_j|\mathrm{data}]} \cdot n_j - n_j, \tag{12}$$

where the above ratio of variances is the direct estimate variance divided by the model posterior variance of μ_j, and n_j is the actual number of plots in hexagon j.

SAE models require careful validation to ensure trustworthy inference. Because the direct estimates, $\hat{\mu}_j$, are design-unbiased, we compare the SFH biomass estimates, given by the posterior mean $\mathrm{E}[\mu_j|\mathrm{data}]$, to the direct estimates to inspect for biases. We evaluate the average difference between the model estimates and the direct estimates, both overall and for high-biomass areas, defined as having a direct estimate greater than 150 Mg/ha. For spatially correlated data, it is difficult to test whether an observed bias is statistically significant. However, point estimates should not be interpreted in isolation, but rather in conjunction with their theoretical errors, such as through credible intervals. Therefore our primary test of the model estimates is to evaluate the rate at which the credible intervals contain the true AGBD.

We conduct a cross-validation study to assess the accuracy of the SFH model and the coverage of the credible intervals. Because a true hexagon AGBD is never observed, we must use the direct estimates as a conduit for our validation. A total of 4296 hexagons have a plot sample size greater than 26. At these sample sizes, we expect the estimated variances of the direct estimates be reliable on their own. This set of large-sample hexagons was randomly partitioned into ten folds. Sequentially, each fold was left out as a test set and the SFH model was trained on the remaining hexagons, including those with sample sizes less than 26. Then a 95% credible interval for each withheld direct estimate is computed. Fig. 4 shows the spatial distribution of test hexagons (hexagons with a sample size greater than 26) used in the cross-validation study. Note that since the test values are direct estimates, $\hat{\mu}_j$, we must consider the sampling error δ_j as well as the modeling error in the construction of the credible interval. Let e_j be the posterior error for test hexagon j such that $\mu_j = \mathrm{E}[\mu_j|\mathrm{data}] + e_j$. Then the direct estimate can be written as

$$\hat{\mu}_j = \mathrm{E}[\mu_j|\mathrm{data}] + e_j + \delta_j. \tag{13}$$

Because hexagon j was withheld from the observed data, posterior error e_j is independent of the sampling error δ_j, so that

$$\mathrm{Var}[\hat{\mu}_j] = \mathrm{Var}[e_j] + \mathrm{Var}[\delta_j]. \tag{14}$$

Ideally, the rate of coverage, or the proportion of test direct estimates contained in the 95% credible intervals, would be approximately 95%. Assuming that the variance of the sampling error, $\mathrm{Var}[\delta_j] = \hat{\sigma}_j^2$, is correct, rates of coverage lower than 95% suggest overly optimistic model uncertainties. Rates of coverage higher than 95% suggest overly conservative model uncertainties. Further, it is important that the coverage remains stable around 95% for all AGBD levels. For instance, it would not be acceptable if coverage for the lower 90% of AGBD values was 98% and the coverage for the upper 10% of AGBD values was 70%, averaging out to 95% coverage: the credible intervals need to be individually interpretable. Thus, we examine the overall coverage and the coverage for hexagons with a direct estimate greater than 150 Mg/ha. We also compare the quantiles of the set of hexagons with a direct estimate contained in the credible interval to the quantiles of the entire direct set. The credible intervals should be equally likely to contain hexagons of any AGBD level, therefore the quantile–quantile plot should follow the one-to-one line.

3. Results

In this section we first present results comparing the area-level predictors from GEDI and NLCD TCC within the SFH model. We compare both the reported model results when fit to the entire data, and their cross-validation performance. We then present results examining the importance of spatial variation in the model by comparing the GEDI model with and without the spatial effects.

3.1. Comparison of GEDI and NLCD TCC as area AGBD predictors

Three different SFH models were fit to all positive-biomass hexagons within CONUS using (1) GEDI alone, (2) TCC alone and (3) both GEDI and TCC as predictors. Fig. 5 summarizes the results, comparing the model estimates and standard deviations to the direct estimates and their standard errors. All three models report significantly better precision than the direct estimates, with the TCC model reporting the lowest standard deviations. However, AGBD estimates of the TCC model are visibly biased low relative to the direct estimates, especially for high-biomass areas. Further, the residuals are skewed high, which defies the model assumptions of normally distributed errors. The models that use GEDI also exhibit some negative bias, but far less than their TCC counterpart. Quantification of this bias is given in the cross-validation study, presented next.

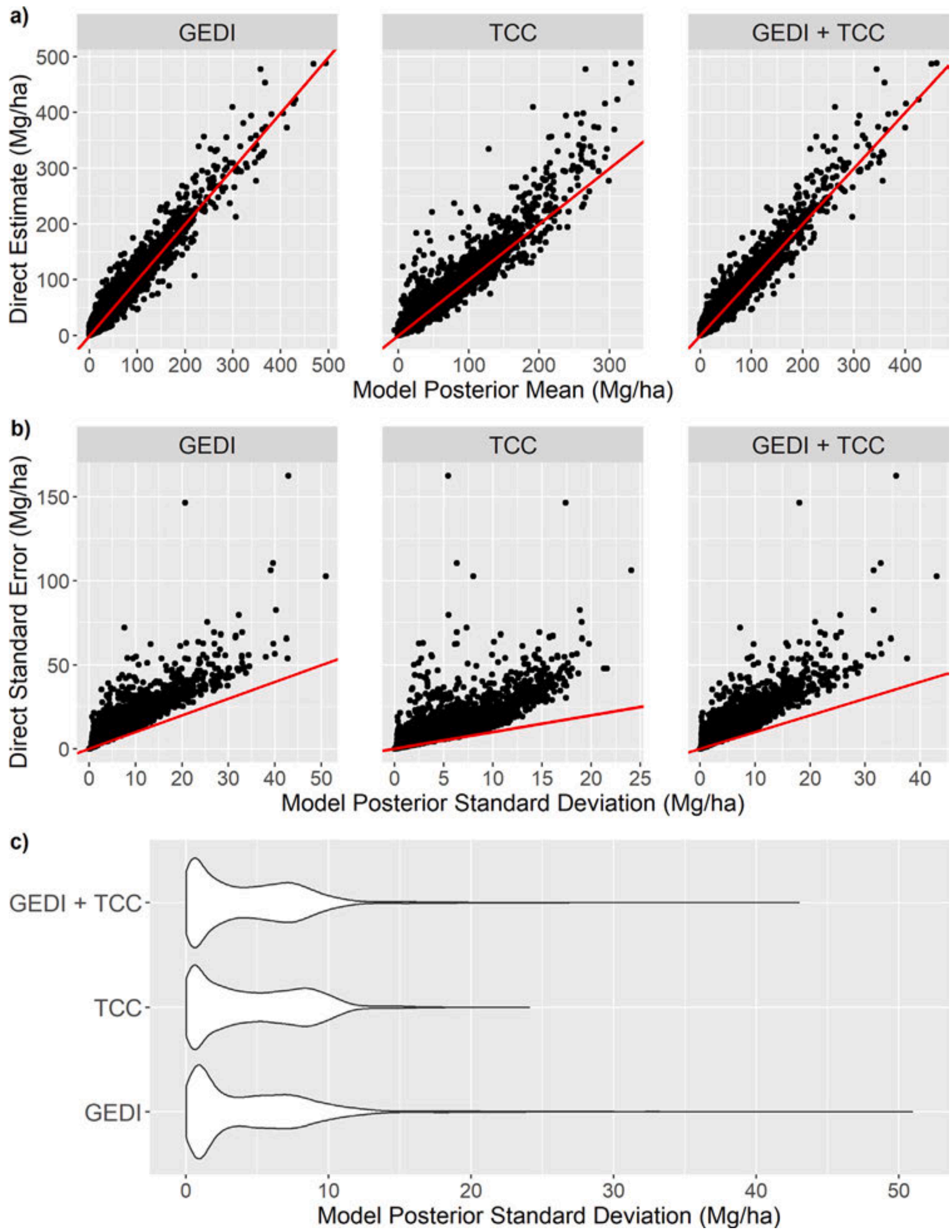

Fig. 5. Model results using GEDI alone, TCC alone, and both GEDI and TCC as predictors. Subfigure (a) gives model estimates versus the direct estimates, (b) gives model standard deviations versus direct standard errors, and (c) gives a violin plot of the distribution of model standard deviations. One-to-one lines are given in red. (For interpretation of the references to color in this figure legend, the reader is referred to the web version of this article.)

To assess the accuracy of the model estimates and uncertainties, we conduct the cross-validation study described in Section 2.6. Fig. 6 and Table 2 give summary plots and statistics from the cross-validation study. All three models had an overall appropriate coverage, with 95% credible intervals containing the withheld direct estimate approximately 95% of the time. But within the 110 test hexagons with a direct estimate greater than 150 Mg/ha, the TCC model 95% credible intervals contained the direct estimate only 80% of the time. The poor coverage implies overly optimistic uncertainties for high-biomass areas. The GEDI models maintain appropriate coverage for the high-biomass areas, suggesting reliable and consistent inference across all biomass levels. The quantile plot in Fig. 6 illustrates this, revealing equal-probability coverage across all biomass levels for the GEDI models and an obvious breakdown in coverage for the TCC alone model for high-biomass areas. The estimates of all three methods exhibit some degree of negative bias relative to the direct estimates, with the bias of the TCC estimates being the most severe. The SFH model using both GEDI and TCC as predictors maintained ideal coverage of the credible intervals while yielding lower standard deviations than the model using GEDI alone. Fig. 7 gives spatial maps of the GEDI + TCC model AGBD estimates and standard deviations for all modeled hexagons, and the effective increases in field plot sample size for hexagons with a direct estimate greater than 50 Mg/ha. Fig. 8 compares the coefficients of variation for the GEDI + TCC model versus those of the direct estimates.

3.2. Importance of spatial variation in the model

Modeling spatial variation was essential to producing reliable inference. For ease of exposition we focus on the GEDI model, though the results are parallel for the other two models. When both the spatially varying coefficient $\tilde{\beta}_j$ and spatial error η_j are included, the GEDI model maintains solid inference at all biomass levels, as demonstrated through

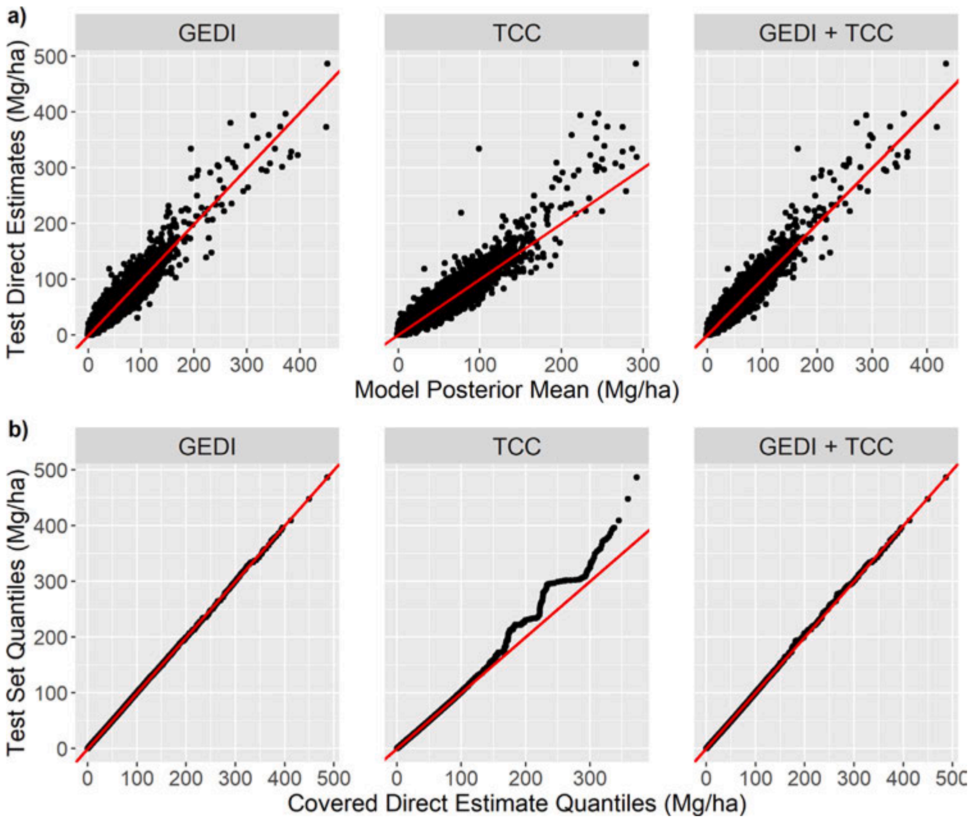

Fig. 6. Cross-validation results using GEDI alone, TCC alone, and both GEDI and TCC as predictors. Subfigure (a) gives the model estimates versus the test direct estimates withheld from the training data. Subfigure (b) gives the quantiles of the test direct estimates covered by the 95% credible intervals versus the quantiles of all test direct estimates. One-to-one lines are given in red. (For interpretation of the references to color in this figure legend, the reader is referred to the web version of this article.)

Table 1
Parameter posterior means for the SFH models using different auxiliary data sources. Spatial range parameters are converted to effective ranges (ER), meaning the distance at which the spatial correlation is 0.05, i.e. essentially uncorrelated. Variance parameters are converted to standard deviation parameters ($\sigma_\beta = \sqrt{\sigma_\beta^2}$), as these have an easier physical interpretation. Parameter uncertainties are not reported here, but aside from intercept μ_0, the uncertainties were slight relative to the magnitude of the posterior means. The magnitude of the non-spatial error, σ_ϵ, was negligibly small for all models, and thus not shown.

Model	μ_0	ER(ϕ_η) (km)	σ_η	β		ER(ϕ_β) (km)		σ_β	
				GEDI	TCC	GEDI	TCC	GEDI	TCC
GEDI	0.39	347	1.78	0.29	–	309	–	0.086	–
TCC	0.56	3190	4.32	–	111.95	–	421	–	63.83
GEDI + TCC	−0.81	1203	1.14	0.16	50.00	439	386	0.074	33.66

the cross-validation study. Removing the spatially varying coefficient drastically reduces the reported standard deviations, with a maximum posterior standard deviation of only 8 Mg/ha. However, it also ruins the coverage at high biomass areas: in the cross-validation study, the coverage of the 95% credible intervals for test hexagons with direct estimates greater than 150 Mg/ha is reduced to 73%. Recall from Section 2.4 that the term $X_j\tilde{\beta}_j$ can also be interpreted as a heteroskedastic spatial error, with variance, $X_j^2\mathrm{Var}[\tilde{\beta}_j]$, increasing with the GEDI predictor X_j. Removing $\tilde{\beta}_j$ from the model leaves all of the unexplained variation to η_j, which has constant variance, causing the model to overestimate the variance in low biomass areas and underestimate the variance in high biomass areas. It is interesting that the structural measurements of GEDI provides not only pertinent information on the AGBD itself, but also on the uncertainty of AGBD estimates. Fig. 9 provides a spatial map of the posterior mean of $X_j\tilde{\beta}_j$ across CONUS. Removing both the spatially varying coefficient and the spatial error, resulting in a traditional Fay–Herriot model, has even worse results. While reporting a maximum standard deviation of only 5 Mg/ha, the coverage of the 95% credible intervals was sub-optimal across all biomass levels (90%), but exceedingly low at high-biomass levels (65%). Additionally, it results in severe spatial bias patterns, due to the lack of any spatial variation in the model. Fig. 10 compares the residuals for the Fay–Herriot model with no spatial effects to the SFH model with the spatial coefficient and error, where residuals are defined as the model posterior mean minus the direct estimates. Table 3 gives summary statistics under the cross-validation study for the GEDI model with spatial effects, $\tilde{\beta}_j$ removed, and both $\tilde{\beta}_j$ and η_j removed.

For all SFH models across the different auxiliary sources, the spatially varying coefficients account for most of the spatial variation in the model. The standard deviation for the spatial error, $\sigma_\eta = \sqrt{\sigma_\eta^2}$, spans between 1.14–4.32 Mg/ha for the different models (Table 1). While the standard deviation for GEDI coefficient, σ_β, may appear small (0.074 for the GEDI + TCC model), this value must be multiplied by the GEDI predictor to yield the contributed deviation to the model. The span of the GEDI predictor values is 0–1740, with a mean of 143, meaning the standard deviation for $X_j\tilde{\beta}_j$ spans from 0–128 Mg/ha, with a mean of 11 Mg/ha for the GEDI + TCC model. The effective range for the spatially varying coefficients (the distance at which the

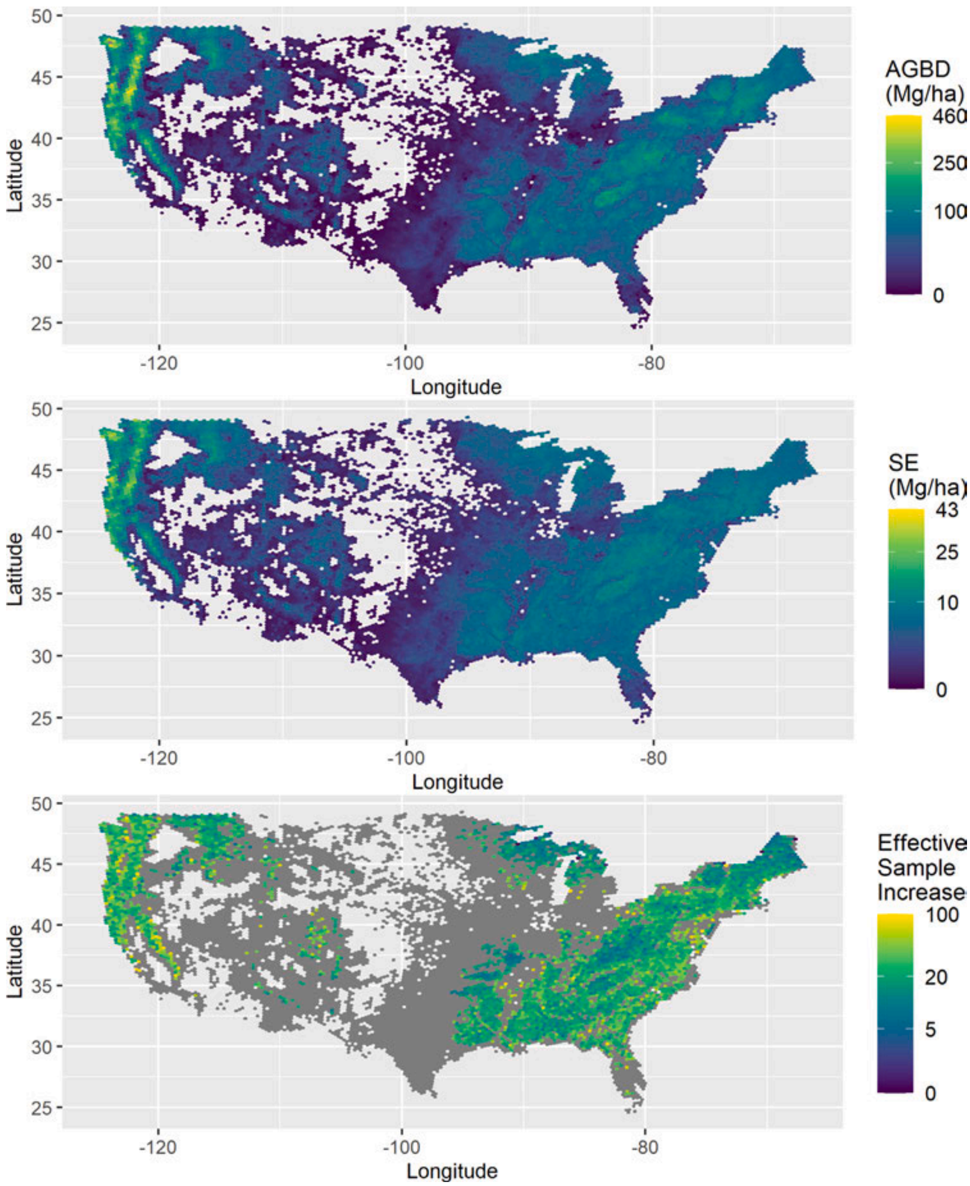

Fig. 7. Spatial maps of the GEDI + TCC model AGBD estimates and standard deviations for all modeled hexagons, and the effective increases in field plot sample size for hexagons with a direct estimate greater than 50 Mg/ha.

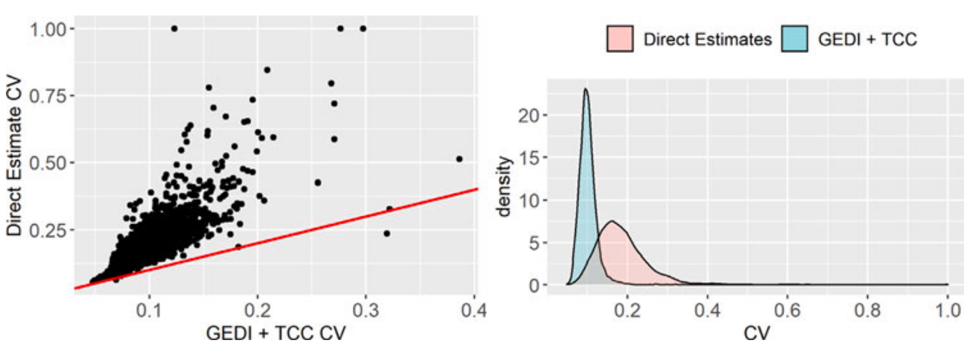

Fig. 8. Coefficients of variation (CV) for the GEDI + TCC model versus the direct estimates. Scatter plot on the left (one-to-one line in red) and density plot on the right. Plots are restricted to hexagons with a direct estimate greater than 50 Mg/ha. The GEDI + TCC model produces substantially lower CVs than the direct estimates.

correlation decreases to 0.05) is between 309–439 km for the different predictors, which is small relative to the size of CONUS, and less than the greatest dimension of many states. This further demonstrates the need for spatially varying models when analyzing large domains and

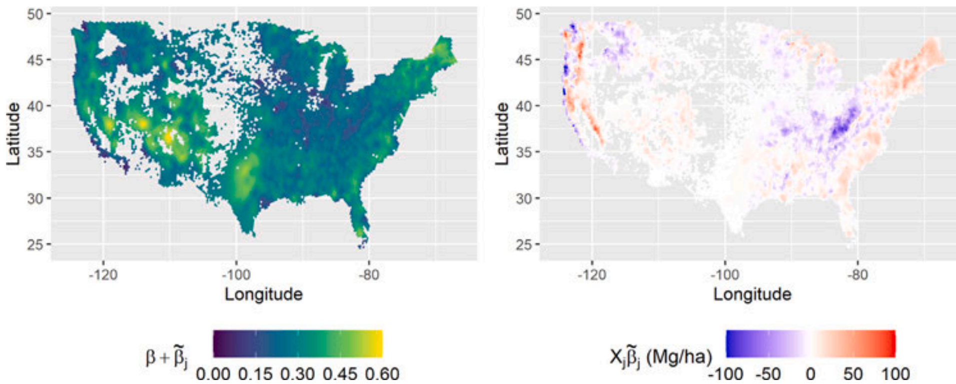

Fig. 9. For the GEDI SFH model, spatial map of the posterior mean of $\beta + \tilde{\beta}_j$ (left), illustrating the variation of the regression coefficient, and spatial map of the posterior mean of $X_j\tilde{\beta}_j$ (right), illustrating the effect of this variation on the model estimates.

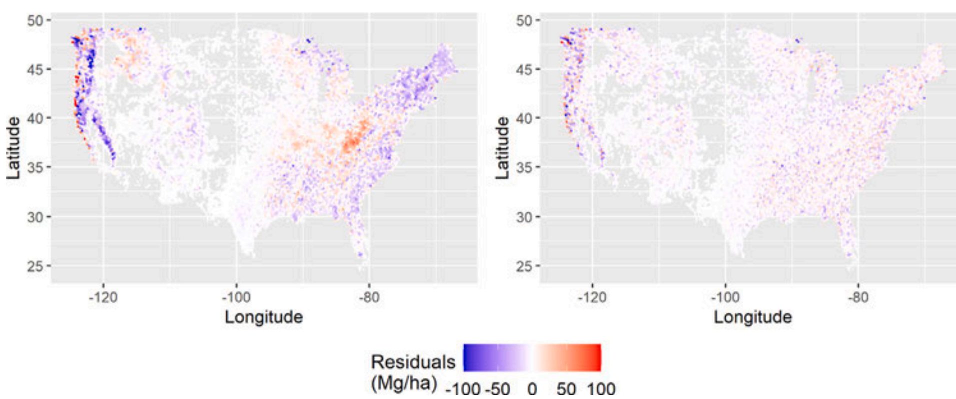

Fig. 10. Using GEDI as a predictor, spatial map of the residuals for the Fay–Herriot model with no spatial effects (left) to the SFH model with the spatial coefficient and error (right), where residuals are defined as the model posterior mean minus the direct estimates.

Table 2
Summary statistics from the cross-validation study comparing auxiliary data sources.

Model	RMSE (Mg/ha)	Mean difference from $\hat{\mu}_j$ (Mg/ha)		95% CI coverage (%)	
		All $\hat{\mu}_j$	$\hat{\mu}_j$ > 150 Mg/ha	All $\hat{\mu}_j$	$\hat{\mu}_j$ > 150 Mg/ha
GEDI	13.14	−2.66	−17.18	95.41	96.36
TCC	15.20	−3.38	−46.09	95.52	80.00
GEDI + TCC	12.70	−2.91	−23.70	95.80	94.55

Table 3
Summary statistics from the cross-validation study comparing the omission of spatial regression coefficient $\tilde{\beta}_j$ and omission of both spatial regression coefficient and spatial error $\tilde{\beta}_j$, η_j.

Model	RMSE (Mg/ha)	Mean difference from $\hat{\mu}_j$ (Mg/ha)		95% CI coverage (%)	
		All $\hat{\mu}_j$	$\hat{\mu}_j$ > 150 Mg/ha	All $\hat{\mu}_j$	$\hat{\mu}_j$ > 150 Mg/ha
GEDI	13.14	−2.66	−17.18	95.41	96.36
GEDI, no $\tilde{\beta}_j$	14.01	−3.62	−38.89	92.52	72.73
GEDI, no $\tilde{\beta}_j$, η_j	16.39	−3.15	−40.05	90.42	65.45

provides a pessimistic example for the geographic transferability of ecological models (Wenger and Olden, 2012; Yates et al., 2018).

4. Discussion

The SFH models using GEDI data produced estimates that significantly reduced the uncertainties of the FIA direct estimates, with improvements comparable to the collection of dozens of additional field plots per hexagon. Considering that such an intensified collection of field plots would be prohibitive in terms of labor and expense, the models presented here provide a powerful tool to enhance the precision of small area forest inventory estimates using publicly available data. Importantly, the cross-validation study shows the credible intervals to have ideal coverage, meaning the reported uncertainty is trustworthy and the credible intervals give an interpretable range of potential AGBD values.

Both the data from GEDI and the NLCD TCC product present potential auxiliary data sources for a SAE model with a broad spatial domain. However, use of the TCC product alone does not produce accurate quantification of uncertainty for high-biomass areas. Even though the reported standard deviations from the TCC model were the lowest, these standard deviations are not meaningful if they produce credible intervals that too often do not contain the true biomass. A parallel discussion can be given to the inclusion/omission of spatial effects. Removing the spatial effects yields incredibly low reported standard deviations, but these standard deviations are not meaningful, as they correspond to credible intervals with poor coverage and therefore do not accurately describe the uncertainty of the model estimates. The comparison of the data sources and inclusion/omission of spatial effects is not only informative for the construction of forestry SAE models, but also presents a more general cautionary example. SAE models must be checked carefully, and simply gravitating to the model with the lowest reported errors without validation is liable to lead to erroneous inference.

The GEDI L4B product contains global predictions of AGBD at a 1 km grid resolution (Dubayah et al., 2022b). Biomass models were trained at the footprint level at a collection of calibration sites, and these footprint-level models are used in conjunction with hybrid estimation to make 1 km resolution predictions of AGBD along with standard errors (Patterson et al., 2019; Duncanson et al., 2022). When compared at identically sized areas, the L4B standard errors are typically substantially lower than those produced from the area-level SAE models presented here. This is because the L4B models are specified and implemented at the footprint level, leading a much higher density of information per area. However, the L4B models exhibit local bias relative to FIA estimates, consistently overestimating AGBD in some locales and underestimating in others. The result is L4B confidence intervals that do not overlap with confidence intervals produced by FIA direct estimates (Dubayah et al., 2022a, Figure 8). Some of this may be attributable to FIA's particular definition of "forest" for which biomass is measured, whereas the GEDI L4B models estimate all above-ground biomass. Still, FIA seeks estimates consistent with their definitions and goals. An SFH model using GEDI and national forest inventory allows the model to adapt across different regions to sparse, but local, field data, rather than extrapolating from a collection of calibration sites. However, this is only applicable in countries with reliable national forest inventories, making it unsuitable to meet the global mandate of GEDI. Interestingly, the spatial bias patterns seen from GEDI L4B (Dubayah et al., 2022a, Figure 8) are strikingly similar to the adjustments from the spatially varying regression coefficient in the right panel of Fig. 9, or the biases of the non-spatial Fay–Herriot in Fig. 10, despite the L4B equations using different GEDI RH metrics and different transformations on both the RH metrics and the biomass density (Duncanson et al., 2022). This suggests these spatial patterns are not artifacts unique to either model, but true variations in the relationship between vertical structural measurements from GEDI and FIA field observations of forest biomass.

Fay–Herriot models cannot ingest direct estimates with a standard error of zero, as occurs here when all of the sampled plots within a hexagon have a measured AGBD of zero. For this reason, all 'zero-biomass' hexagons were omitted from the analysis, which is not necessarily desirable. This issue could be addressed with zero-inflated models, which simultaneously model the proportion of zeros and the magnitude of the non-zeros (Finley et al., 2011; Chandra and Sud, 2012; Bocci et al., 2020). Such models would address a shortcoming of both the SFH (which necessitates omission of the zero-biomass areas) and the direct design-based estimates (which give an estimated standard error of zero for these areas).

The SFH model, and other area-level SAE models, require the small areas to be defined prior to model fitting. In our study, the small areas were defined as the 64,000 hectare hexagons. While it is simple to make estimates of small area aggregates after model fitting, e.g. compute average AGBD for all hexagons in California, it is impossible to make estimates for areas not composed of the pre-defined small areas. Therefore it is recommended to fit the model at the finest resolution desired (or possible) and then compute estimates for any area aggregates desired. It would be an interesting study to examine the performance of an area-level SAE model under increasingly fine resolutions. Certainly, at some point the majority of small areas would contain few or no field plots, rendering the direct estimates meaningless. But it is possible that some other model component would break down first, perhaps assumptions of normality or the linear relationship with the predictor. These limitations in resolution may inhibit the usefulness of our data and methods for land managers. Many forest management decisions occur at the stand level (Yoshimoto et al., 2016). While the sampling density of GEDI may be fine enough to make its observations a viable, and perhaps powerful, area-level predictor for many stands, the base sampling density of FIA is such that the vast majority of stands will contain at most one, but more likely no field plots. Therefore the stands will have no direct estimate, a necessary starting point for Fay–Herriot models. Fay–Herriot models have been successfully used to improve stand-level estimates (Ver Planck et al., 2018; Temesgen et al., 2021), but these studies utilized field plots sampled at a far greater density than those of FIA.

An implementation of a unit-level SAE model relating individual GEDI footprints to individual field plots is appealing due to the far greater density of leveraged information. Furthermore, a unit-level model would not require the small areas to be defined before model training, and any area containing sampled GEDI footprints could be given an estimate, e.g. a forest stand. Such an implementation faces obstacles, however. First, assumptions of normally distributed errors which are tenable for area aggregates are often not at the plot-level. Next, aggregating to the area level provides a convenient way to circumvent the spatial misalignment of the GEDI footprints and field plots. This misalignment is further complicated by the geolocation accuracy of GEDI footprints (standard error of around 10 m), and perhaps also geolocation accuracy of the field plots.

5. Conclusion

We implemented an area-level SAE model with spatial variation to estimate forest AGBD within 64,000 ha hexagons across CONUS. Two different predictors, derived from GEDI and the NLCD 2016 TCC product respectively, were compared for their resulting model performance. The models that used the GEDI-derived predictors resulted in reliable inference across all biomass levels with substantially better precision than direct estimates using field data alone. The model that used the TCC product alone reported better precision than the direct estimates and the GEDI models, but the cross-validation study showed this reported precision to be unrealistic. We demonstrated that accounting for spatial variation in the model was crucial for trustworthy inference, and that not doing so resulted in clear local bias patterns and poor quantification of uncertainty. The implications of this work are threefold: first, we have produced a biomass map consistent with FIA data and current estimates with higher precision than the current estimates. More generally, we demonstrated an effective model and auxiliary data source for forestry small area estimates. Finally, and most generally, the results emphasize the importance of carefully validating SAE models.

CRediT authorship contribution statement

Paul May: Conceptualization, Methodology, Software, Validation, Formal analysis, Writing – original draft. **Kelly S. McConville:** Conceptualization, Writing – review & editing. **Gretchen G. Moisen:** Conceptualization, Writing – review & editing. **Jamis Bruening:** Data curation, Software, Writing – review & editing. **Ralph Dubayah:** Writing – review & editing, Supervision, Project administration, Funding acquisition.

Declaration of competing interest

The authors declare that they have no known competing financial interests or personal relationships that could have appeared to influence the work reported in this paper.

Data availability

Data and 'R' code to reproduce the results in this work are available on Mendeley Data, DOI: 10.17632/z2wj33w435.1

Acknowledgments

This research was supported by NASA Contract, United States [#NNL15AA03C] for the development and execution of the GEDI mission (May, Dubayah, Bruening), a NASA FINESST Fellowship, United States [#80NSSC21K1626] (Dubayah, Bruening), and a NASA Applications Supplement to a grant from NASA's Carbon Monitoring System, United States [#80NSSC20K0023] (Dubayah, May). We thank John Armston at the University of Maryland - College Park for his assistance with GEDI data access and Tracey Frescino at the US Forest Service for compiling the FIA plot data used in the study.

References

Babcock, Chad, Finley, Andrew O., Andersen, Hans-Erik, Pattison, Robert, Cook, Bruce D., Morton, Douglas C., Alonzo, Michael, Nelson, Ross, Gregoire, Timothy, Ene, Liviu, Gobakken, Terje, Næsset, Erik, 2018. Geostatistical estimation of forest biomass in interior Alaska combining Landsat-derived tree cover, sampled airborne LiDAR and field observations. Remote Sens. Environ. (ISSN: 0034-4257) 212, 212–230. http://dx.doi.org/10.1016/j.rse.2018.04.044, URL https://www.sciencedirect.com/science/article/pii/S0034425718302013.

Bechtold, William A., Patterson, Paul L., 2005. The Enhanced Forest Inventory and Analysis Program–National Sampling Design and Estimation Procedures, no. 80. USDA Forest Service, Southern Research Station.

Bocci, Chiara, Dreassi, Emanuela, Petrucci, Alessandra, Rocco, Emilia, 2020. Small area estimation for skewed semicontinuous spatially structured responses. In: Statistical Methods and Applications in Forestry and Environmental Sciences. Springer, pp. 241–253.

Breidenbach, Johannes, Magnussen, Steen, Rahlf, Johannes, Astrup, Rasmus, 2018. Unit-level and area-level small area estimation under heteroscedasticity using digital aerial photogrammetry data. Remote Sens. Environ. (ISSN: 0034-4257) 212, 199–211. http://dx.doi.org/10.1016/j.rse.2018.04.028, URL https://www.sciencedirect.com/science/article/pii/S0034425718301858.

Cao, Qianqian, Dettmann, Garret T., Radtke, Philip J., Coulston, John W., Derwin, Jill, Thomas, Valerie A., Burkhart, Harold E., Wynne, Randolph H., 2022. Increased precision in county-level volume estimates in the United States National Forest inventory with area-level small area estimation. Front. For. Glob. Change (ISSN: 2624-893X) 5, URL https://www.frontiersin.org/article/10.3389/ffgc.2022.769917.

Chandra, Hukum, Salvati, Nicola, Chambers, Ray, 2015. A spatially nonstationary Fay-Herriot model for small area estimation. J. Surv. Stat. Methodol. (ISSN: 2325-0984) 3 (2), 109–135. http://dx.doi.org/10.1093/jssam/smu026.

Chandra, Hukum, Sud, U.C., 2012. Small area estimation for zero-inflated data. Comm. Statist. Simulation Comput. 41 (5), 632–643.

Coulston, John W., Moisen, Gretchen G., Wilson, Barry T., Finco, Mark V., Cohen, Warren B., Brewer, C. Kenneth, 2012. Modeling percent tree Canopy cover: A pilot study. Photogramm. Eng. Remote Sens. 78 (7), 715–727.

Cressie, Noel, 2015. Statistics for Spatial Data. John Wiley & Sons.

Datta, Abhirup, Banerjee, Sudipto, Finley, Andrew O., Gelfand, Alan E., 2016. Hierarchical nearest-neighbor Gaussian process models for large geostatistical datasets. J. Amer. Statist. Assoc. 111 (514), 800–812.

Dewitz, J., 2021. National Land Cover Database (NLCD) 2019 Products. Technical Report Version 2, U.S. Geological Survey, http://dx.doi.org/10.5066/P9KZCM54.

Dubayah, Ralph, Armston, John, Healey, Sean, Bruening, Jamis, Patterson, Paul, Kellner, James, Duncanson, Laura, Saarela, Svetlana, Ståhl, Göran, Yang, Zhiqiang, Tang, Hao, Blair, J. Bryan, Fatoyinbo, Lola, Goetz, Scott, Hancock, Steven, Hansen, Matt, Hofton, Michelle, Hurtt, George, Luthcke, Scott, 2022a. GEDI launches a new era of biomass inference from space. URL https://eartharxiv.org/repository/view/3278/, Publisher: EarthArXiv.

Dubayah, R., Armston, J., Healey, S., Yang, Z., Patterson, P., Saarela, S., Stahl, G., Duncanson, L., Kellner, J., 2022b. GEDI L4B gridded aboveground biomass density, Version 2 [Data set]. http://dx.doi.org/10.3334/ORNLDAAC/2017, ORNL DAAC, Oak Ridge, Tennessee, USA.

Dubayah, Ralph, Blair, James Bryan, Goetz, Scott, Fatoyinbo, Lola, Hansen, Matthew, Healey, Sean, Hofton, Michelle, Hurtt, George, Kellner, James, Luthcke, Scott, Armston, John, Tang, Hao, Duncanson, Laura, Hancock, Steven, Jantz, Patrick, Marselis, Suzanne, Patterson, Paul L., Qi, Wenlu, Silva, Carlos, 2020a. The global ecosystem dynamics investigation: High-resolution laser ranging of the earth's forests and topography. Sci. Remote Sens. (ISSN: 2666-0172) 1, 100002. http://dx.doi.org/10.1016/j.srs.2020.100002, URL https://www.sciencedirect.com/science/article/pii/S2666017220300018.

Dubayah, R., Hofton, M., Blair, J., Armston, J., Tang, H., Luthcke, S, 2020b. GEDI L2A elevation and height metrics data global footprint level V001 [Data set]. http://dx.doi.org/10.5067/GEDI/GEDI02_A.001, NASA EOSDIS Land Processes DAAC.

Duncanson, Laura, Kellner, James R., Armston, John, Dubayah, Ralph, Minor, David M., Hancock, Steven, Healey, Sean P., Patterson, Paul L., Saarela, Svetlana, Marselis, Suzanne, Silva, Carlos E., Bruening, Jamis, Goetz, Scott J., Tang, Hao, Hofton, Michelle, Blair, Bryan, Luthcke, Scott, Fatoyinbo, Lola, Abernethy, Katharine, Alonso, Alfonso, Andersen, Hans-Erik, Aplin, Paul, Baker, Timothy R., Barbier, Nicolas, Bastin, Jean Francois, Biber, Peter, Boeckx, Pascal, Bogaert, Jan, Boschetti, Luigi, Boucher, Peter Brehm, Boyd, Doreen S., Burslem, David F.R.P., Calvo-Rodriguez, Sofia, Chave, Jérôme, Chazdon, Robin L., Clark, David B., Clark, Deborah A., Cohen, Warren B., Coomes, David A., Corona, Piermaria, Cushman, K.C., Cutler, Mark E.J., Dalling, James W., Dalponte, Michele, Dash, Jonathan, de Miguel, Sergio, Deng, Songqiu, Ellis, Peter Woods, Erasmus, Barend, Fekety, Patrick A., Fernandez-Landa, Alfredo, Ferraz, Antonio, Fischer, Rico, Fisher, Adrian G., García-Abril, Antonio, Gobakken, Terje, Hacker, Jorg M., Heurich, Marco, Hill, Ross A., Hopkinson, Chris, Huang, Huabing, Hubbell, Stephen P., Hudak, Andrew T., Huth, Andreas, Imbach, Benedikt, Jeffery, Kathryn J., Katoh, Masato, Kearsley, Elizabeth, Kenfack, David, Kljun, Natascha, Knapp, Nikolai, Král, Kamil, Krůček, Martin, Labrière, Nicolas, Lewis, Simon L., Longo, Marcos, Lucas, Richard M., Main, Russell, Manzanera, Jose A., Martínez, Rodolfo Vásquez, Mathieu, Renaud, Memiaghe, Herve, Meyer, Victoria, Mendoza, Abel Monteagudo, Monerris, Alessandra, Montesano, Paul, Morsdorf, Felix, Næsset, Erik, Naidoo, Laven, Nilus, Reuben, O'Brien, Michael, Orwig, David A., Papathanassiou, Konstantinos, Parker, Geoffrey, Philipson, Christopher, Phillips, Oliver L., Pisek, Jan, Poulsen, John R., Pretzsch, Hans, Rüdiger, Christoph, Saatchi, Sassan, Sanchez-Azofeifa, Arturo, Sanchez-Lopez, Nuria, Scholes, Robert, Silva, Carlos A., Simard, Marc, Skidmore, Andrew, Stereńczak, Krzysztof, Tanase, Mihai, Torresan, Chiara, Valbuena, Ruben, Verbeeck, Hans, Vrska, Tomas, Wessels, Konrad, White, Joanne C., White, Lee J.T., Zahabu, Eliakimu, Zgraggen, Carlo, 2022. Aboveground biomass density models for NASA's global ecosystem dynamics investigation (GEDI) LiDAR mission. Remote Sens. Environ. (ISSN: 00344257) 270, 112845. http://dx.doi.org/10.1016/j.rse.2021.112845, URL https://linkinghub.elsevier.com/retrieve/pii/S0034425721005654.

Fay, Robert E., Herriot, Roger A., 1979. Estimates of income for small places: An application of James-Stein procedures to census data. J. Amer. Statist. Assoc. (ISSN: 0162-1459) 74 (366), 269–277. http://dx.doi.org/10.2307/2286322, URL https://www.jstor.org/stable/2286322, Publisher: [American Statistical Association, Taylor & Francis, Ltd.].

Finley, Andrew O., Banerjee, Sudipto, MacFarlane, David W., 2011. A hierarchical model for quantifying forest variables over large heterogeneous landscapes with uncertain forest areas. J. Amer. Statist. Assoc. 106 (493), 31–48.

Gelfand, Alan E., Kim, Hyon-Jung, Sirmans, C.F., Banerjee, Sudipto, 2003. Spatial modeling with spatially varying coefficient processes. J. Amer. Statist. Assoc. 98 (462), 387–396.

Genton, Marc G., 2001. Classes of kernels for machine learning: A statistics perspective. J. Mach. Learn. Res. 2 (Dec), 299–312.

Green, P. Corey, Burkhart, Harold E., Coulston, John W., Radtke, Philip J., 2020. A novel application of small area estimation in loblolly pine forest inventory. Forestry: Int. J. For. Res. (ISSN: 0015-752X) 93 (3), 444–457. http://dx.doi.org/10.1093/forestry/cpz073.

Gregoire, T.G., 1998. Design-based and model-based inference in survey sampling: Appreciating the difference. Can. J. Forest Res. (ISSN: 0045-5067) 28 (10), 1429–1447. http://dx.doi.org/10.1139/x98-166, URL https://cdnsciencepub.com/doi/10.1139/x98-166, Publisher: NRC Research Press.

Horvitz, Daniel G., Thompson, Donovan J., 1952. A generalization of sampling without replacement from a finite universe. J. Amer. Statist. Assoc. 47 (260), 663–685.

Lindgren, Finn, Rue, Håvard, 2015. Bayesian spatial modelling with R-INLA. J. Stat. Softw. (ISSN: 1548-7660) 63, 1–25. http://dx.doi.org/10.18637/jss.v063.i19.

Marhuenda, Yolanda, Molina, Isabel, Morales, Domingo, 2013. Small area estimation with spatio-temporal Fay–Herriot models. Comput. Statist. Data Anal. (ISSN: 0167-9473) 58, 308–325. http://dx.doi.org/10.1016/j.csda.2012.09.002, URL https://www.sciencedirect.com/science/article/pii/S0167947312003222.

Menlove, J., Healey, S.P., 2021. Carbon monitoring system (CMS)CMS: Forest aboveground biomass from FIA plots across the conterminous USA, 2009–2019. p. 0 MB. http://dx.doi.org/10.3334/ORNLDAAC/1873, URL https://daac.ornl.gov/cgi-bin/dsviewer.pl?ds_id=1873, Artwork Size: 0 MB Medium: KMZ Shapefile, ESRI Shapefile Publisher: ORNL Distributed Active Archive Center Version Number: 1.

Patterson, Paul L., Healey, Sean P., Ståhl, Göran, Saarela, Svetlana, Holm, Sören, Andersen, Hans-Erik, Dubayah, Ralph O., Duncanson, Laura, Hancock, Steven, Armston, John, Kellner, James R., Cohen, Warren B., Yang, Zhiqiang, 2019. Statistical properties of hybrid estimators proposed for GEDI—NASA's global ecosystem dynamics investigation. Environ. Res. Lett. (ISSN: 1748-9326) 14 (6), 065007. http://dx.doi.org/10.1088/1748-9326/ab18df, Publisher: IOP Publishing.

Pratesi, Monica, Salvati, Nicola, 2008. Small area estimation: The EBLUP estimator based on spatially correlated random area effects. Stat. Methods Appl. (ISSN: 1613-981X) 17 (1), 113–141. http://dx.doi.org/10.1007/s10260-007-0061-9.

Prisley, Steve, Bradley, Jeff, Clutter, Mike, Friedman, Suzy, Kempka, Dick, Rakestraw, Jim, Sonne Hall, Edie, 2021. Needs for small area estimation: Perspectives from the US private forest sector. Front. For. Glob. Change (ISSN: 2624-893X) 4, URL https://www.frontiersin.org/article/10.3389/ffgc.2021.746439.

R. Core Team, 2021. R: A language and environment for statistical computing. R Foundation for Statistical Computing, Vienna, Austria, URL https://www.R-project.org/.

Rao, J.N.K., Molina, Isabel, 2015. Small Area Estimation. John Wiley & Sons, ISBN: 978-1-118-73578-7, Google-Books-ID, i1B_BwAAQBAJ.

Rue, Håvard, Martino, Sara, Chopin, Nicolas, 2009. Approximate Bayesian inference for latent Gaussian models by using integrated nested Laplace approximations. J. R. Stat. Soc. Ser. B Stat. Methodol. (ISSN: 1467-9868) 71 (2), 319–392. http://dx.doi.org/10.1111/j.1467-9868.2008.00700.x, URL https://onlinelibrary.wiley.com/doi/abs/10.1111/j.1467-9868.2008.00700.x, _eprint: https://onlinelibrary.wiley.com/doi/pdf/10.1111/j.1467-9868.2008.00700.x.

Särndal, Carl-Erik, Thomsen, Ib, Hoem, Jan M., Lindley, D.V., Barndorff-Nielsen, O., Dalenius, Tore, 1978. Design-based and model-based inference in survey sampling [with discussion and reply]. Scand. J. Stat. (ISSN: 0303-6898) 5 (1), 27–52, URL https://www.jstor.org/stable/4615682, Publisher: [Board of the Foundation of the Scandinavian Journal of Statistics, Wiley].

Temesgen, Hailemariam, Mauro, Francisco, Hudak, Andrew T., Frank, Bryce, Monleon, Vicente, Fekety, Patrick, Palmer, Marin, Bryant, Timothy, 2021. Using Fay-Herriot models and variable radius plot data to develop a stand-level inventory and update a prior inventory in the western Cascades, OR, United States. Front. For. Glob. Change. 4: 745916 4, 745916. http://dx.doi.org/10.3389/ffgc.2021.745916, URL http://www.fs.usda.gov/treesearch/pubs/63846.

Ver Planck, Neil R., Finley, Andrew O., Kershaw, John A., Weiskittel, Aaron R., Kress, Megan C., 2018. Hierarchical Bayesian models for small area estimation of forest variables using LiDAR. Remote Sens. Environ. (ISSN: 0034-4257) 204, 287–295. http://dx.doi.org/10.1016/j.rse.2017.10.024, URL https://www.sciencedirect.com/science/article/pii/S0034425717304868.

Wenger, Seth J., Olden, Julian D., 2012. Assessing transferability of ecological models: An underappreciated aspect of statistical validation. Methods Ecol. Evol. 3 (2), 260–267.

White, Grayson W., McConville, Kelly S., Moisen, Gretchen G., Frescino, Tracey S., 2021. Hierarchical Bayesian small area estimation using weakly informative priors in ecologically homogeneous areas of the interior western forests. Front. For. Glob. Change (ISSN: 2624-893X) 4, URL https://www.frontiersin.org/article/10.3389/ffgc.2021.752911.

Wiener, Sarah S., Bush, Renate, Nathanson, Amy, Pelz, Kristen, Palmer, Marin, Alexander, Mara L., Anderson, David, Treasure, Emrys, Baggs, Joanne, Sheffield, Ray, 2021. United States forest service use of forest inventory data: Examples and needs for small area estimation. Front. For. Glob. Change (ISSN: 2624-893X) 4, URL https://www.frontiersin.org/article/10.3389/ffgc.2021.763487.

Yang, Limin, Jin, Suming, Danielson, Patrick, Homer, Collin, Gass, Leila, Bender, Stacie M, Case, Adam, Costello, Catherine, Dewitz, Jon, Fry, Joyce, et al., 2018. A new generation of the United States national land cover database: Requirements, research priorities, design, and implementation strategies. ISPRS J. Photogramm. Remote Sens. 146, 108–123.

Yates, Katherine L., Bouchet, Phil J., Caley, M. Julian, Mengersen, Kerrie, Randin, Christophe F., Parnell, Stephen, Fielding, Alan H., Bamford, Andrew J., Ban, Stephen, Barbosa, A. Márcia, et al., 2018. Outstanding challenges in the transferability of ecological models. Trends Ecol. Evol. 33 (10), 790–802.

Yoshimoto, Atsushi, Asante, Patrick, Konoshima, Masashi, 2016. Stand-level forest management planning approaches. Curr. For. Rep. 2 (3), 163–176.